

School of Physics and Astronomy
Queen Mary University of London

Theories and Models of Dark Energy

Saashiv Valjee (190288688)

June 15, 2023

Supervisor: Dr Chris Clarkson

SPA6913-B Extended Independent Project
15 Credit Units

Submitted in partial fulfilment of the requirements for the degree of
MSci FT AstroPhysics from Queen Mary University of London

Abstract

Throughout our time trying to study and understand Dark Energy, many theories have surfaced, some of which have become much more popular than others. This report aims to cover a wider range of theories surrounding Dark Energy including the idea behind the theory, mathematical proofs for such theories and whether the theories could be considered as realistic candidates.

Contents

List of Figures	1
1 Introduction	2
2 Equation of State for Dark Energy	3
3 Observational Evidence Supporting Dark Energy	4
3.1 Age of the Universe	4
3.2 Supernovae	5
3.3 CMB	7
3.4 BAO	9
3.5 Large-Scale Structure	10
4 Statistical Methods in Cosmology	11
4.1 The likelihood function	11
4.2 Fisher Matrix	14
5 Dark Energy Constraints	17
5.1 parameterization of w_{DE}	17
5.2 Supernova Ia data	19
5.3 Constraints on CMB	21
5.4 The cross Correlation	22
6 Models	24
6.1 Cosmological Constant	24
6.2 Dark Energy models with Scaling Solutions	26
6.3 Quintessence	27
6.4 K-Essence	29
6.5 Phantom Fields	31
6.5.1 Constant δ Models	34
6.5.2 Varying δ Models	34
6.6 Tachyon Fields	37

6.7	Chameleon Scalar Fields	39
6.8	Chaplygin Gas	41
6.9	Unified Models of Dark Energy and Dark Matter	43
6.9.1	Generalized Chaplygin Gas	43
6.9.2	K-essence as a unified model	44
6.10	Future Singularities	46
7	Conclusion	49
	Bibliography	50

List of Figures

3.1	The CMB power spectrum versus the multiple moment and angular size. This curve shows the theoretical prediction of the power spectrum while the black points represent the WMAP data spanning across 5 years.	8
3.2	This graph displays the large scale redshift space correlation function of the SDSS sample of data. The smaller graph shows a zoomed-in version of the main graph, at the peak observed at $100h^{-1}Mpc$. From top to bottom, each curvature corresponds to $\Omega_m^{(0)}h^2 = 0.12, 0.13, 0.14$, with $\Omega_b^{(0)}h^2 = 0.024$. A pure CDM (baryon-less) model with $\Omega_m^{(0)}h^2 = 0.15$. The data clearly shows the acoustic peak around the stated separation distance.[1]	9
3.3	The predicted power mater power spectrum in the flat Λ CDM model, plotted along side the CDM model.	10
5.1	Plot displays the evolution of the equation of state for dark every for the best-fit of the Kink parameterization. The maximized limits on $w(z)$ are displayed as redshift: the red dashed line, scale factor: green dashed and dotted line, logarithmic: blue dotted line, Kink: solid black lines	19

1 Introduction

Dark energy was discovered in 1998 and since then, hundreds and thousands of papers have been written aiming to cover its potential forms and explain its behaviour. It started in 1917 when Einstein added the cosmological constant to the field equations which gives a static universe. 3 years later, Pauli had a realization that for a radiation field, the vacuum energy is too large to gravitate. In 1931, Einstein decided to remove the cosmological constant due to cosmic expansions discovery (as he had added it in to obtain a static universe). Fast forward to 1967, Zeldovich wanted to reintroduce the cosmological constant by considering vacuum fluctuations. This created the "Fine Tuning" problem. A whole 20 years later, Weinberg predicted a non-vanishing small cosmological constant, and had it published another 2 years later. In 1998, finally, the acceleration of the expanding universe was discovered due to analysis from Type Ia supernova data. This paper aims to review the many concepts surrounding and connected to dark energy including: The observational evidence that supports its existence, the statistical methods that can be used to analyse data, the constraints we have on dark energy, and some of the (many) models of dark energy. We will conclude by surveying the models and deducing which model best describes the observable behaviour.

[7, p. 2]

2 Equation of State for Dark Energy

If we imagine dark energy with the equation of state $w_{DE} = P_{DE}/\rho_{DE}$, that satisfies the continuity equation:

$$\dot{\rho}_{DE} + 3H(\rho_{DE} + P_{DE}) = 0 \quad (2.1)$$

which can be integrated using: $-dt = dz/H(z+1)$, we can obtain an expression for the density of dark energy:

$$\rho_{DE} = \rho_{DE}^{(0)} a^{-3(1+w_{DE})} \quad (2.2)$$

By stating that the sum of the energy densities must equal 1, our Friedmann equation becomes:

$$H^2(a) = H_0^2(\Omega_m a^{-3} + \Omega_r a^{-4} + \Omega_k a^{-2} + \Omega_{DE} a^{-3(1+w_{DE})}) \quad (2.3)$$

This can be rearranged to find the equation of state for dark energy.

[3, p. 22-25]

3 Observational Evidence

Supporting Dark Energy

3.1 Age of the Universe

By accepting that the oldest stellar object we've discovered must still be younger than the universe, the fact that dark energy (or something similar) exists, must also be accepted. To demonstrate; take a flat universe where $\Omega_k = 0$. By setting the cosmological constant to 0, we can calculate the age of a universe without dark energy. Using (2.3), and the fact that $a = 1/(1+z)$. we can compute:

$$t_0 = \int_0^\infty \frac{dz}{H(1+z)} \quad (3.1)$$

to calculate the age of this universe:

$$t_0 = \int_0^\infty (H_0^2(\Omega_m(1+z)^3 + \Omega_r(1+z)^4 + \Omega_k(1+z)^2 + \Omega_{DE}(1+z)^{3(1+w_{DE})}))^{-1} dz \quad (3.2)$$

$$\Omega_r = 0 \text{ (insignificant)}$$

$$\Omega_{DE} = 0 \text{ (not present)}$$

$$\Omega_k = 0 \text{ (flat universe)}$$

$$\Omega_m = 1 \text{ (Energy density sum rule)}$$

$$t_0 = \frac{2}{3H_0} \quad (3.3)$$

The Hubble parameter is estimated to be around $H_0^{-1} = 9.776h^{-1}\text{Gyr}$, $0.64 < h < 0.80$. This makes the universe we've imagined roughly 8 to 10Gyrs old, while the oldest object in space is roughly 13Gyrs old. Clearly, there is an issue with this universe, where the only major difference between it and ours is Dark Energies existence.

[3, p. 84-87] [5, p. 10-12]

3.2 Supernovae

Supernovae act as standard candles, which are stellar objects with known brightness. This is useful as we can relate their known brightness to their observed redshift to easily calculate their distance and age (without knowing their luminosity, this is much much harder to do). A type 1a supernova occurs in binary systems including white dwarfs, where the white dwarfs mass increases past the Chandrasekhar limit. The reason we know their luminosity is because we believe that they are formed in the same way regardless of their location. By using:

$$d_L(z) \frac{z}{H_0}, z < 1 \quad (3.4)$$

and data from [4], we can calculate an estimate for the luminosity distance and compare it to theoretical values in universes with a similar composition to ours, and ones without dark energy. SN1998fc had a redshift of 0.10 and an apparent magnitude of 20.5. This makes it's luminosity distance roughly 1428.6pc (using H_0 as 70). The generalised equation for luminosity distance is:

$$d_L^2 = \frac{L_s}{4\pi F} \quad (3.5)$$

Where L_s is the absolute luminosity and F is the energy flux. Light moving in the χ direction must satisfy the geodesic equation:

$$ds^2 = -dt^2 + a^2(t)d\chi^2 = 0 \quad (3.6)$$

From this, we obtain:

$$\chi_s = \int_0^{\chi_s} d\chi = \int_{t_1}^{t_0} \frac{dt}{a(t)} = \frac{1}{a_0 H_0} \int_0^z \frac{dz'}{h(z')} \quad (3.7)$$

Where $h(z) = \frac{H(z)}{H_0}$. The FRW metric is given by:

$$ds^2 = -dt^2 + a^2(t) \left[\frac{dr^2}{1 - Kr^2} + r^2(d\theta + r^2(d\theta^2 + \sin^2\theta d\phi^2)) \right] \quad (3.8)$$

which can also be written as:

$$ds^2 = -dt^2 + a^2(t) \left[d\chi^2 + f_k^2(\chi)(d\theta + r^2(d\theta^2 + \sin^2\theta d\phi^2)) \right] \quad (3.9)$$

While $f_k(\chi)$ varies between $\sin(\chi)$, χ , $\sinh(\chi)$ for $K = 1, 0$ and -1

Using (3.9), we can find the surface area of a sphere at $t = t_0$ and get:

$$F = \frac{L_0}{4\pi(a_0 f_k(x_s))^2} \quad (3.10)$$

which then gives us an equation for Luminosity distance:

$$d_L = a_0 f_k(\chi_s)(1 + z) \quad (3.11)$$

In a flat FRW background with $f_k(\chi) = \chi$ we get:

$$d_L = \frac{1 + z}{H_0} \int_0^z \frac{dz'}{h(z')} \quad (3.12)$$

We can now express $H(z)$ in terms of d_L :

$$H(z) = \frac{d}{dz} \left(\frac{d_L(z)}{1 + z} \right)^{-1} \quad (3.13)$$

And finally, d_L in terms of the energy densities:

$$d_L = \frac{1 + z}{H_0} \int_0^z \frac{1}{\sqrt{\sum_i \Omega_i (1 + z')^{3(1+w_i)}}} dz' \quad (3.14)$$

Using this equation, we can examine which set of values for energy densities fits the data for the supernova. Using $\Omega_m = 1$ we obtain $d_L = 1823.25pc$, while using $\Omega_m = 0.3, \Omega_\Lambda = 0.7$ we get $d_L = 1578.8pc$ which is significantly closer to the practical value received earlier (1428.6pc). Thus, the supernova data has also aided in showing Dark Energy exists. Note that in [5], not only did their estimates show the same relation, but their estimate for 2 energy densities was also above their practical value by 6% while this value was above by roughly 10%. This effect has been detected and therefore shows Dark energy (or something similar) exists.

[5, p. 9][3, p. 87-92]

3.3 CMB

The Sachs-Wolfe Effect causes the photons in CMB to be gravitational redshifted. The integrated Sachs-Wolfe (ISW) effect comes from gravitational redshift as well. Although, it's observed in-between the surface of last-scattering and Earth. Therefore, it's nowhere to be found in the primordial CMB. Rather than that, its effects can be expected when the universe's energy density is dominated by something other than matter. If the universe is matter-dominated, large scale gravitational potential energy wells don't evolve. Otherwise, they will grow and slightly change the energy of the photons passing through them.

The late time ISW effect has arisen due to the way Dark energy controls the growth of the universe. The accelerated expansion due to dark energy causes large-scale potential wells like super-clusters, and hills like voids, to decay over the time it takes a photon to travel through them. Upon entering the super-cluster, the photon gains energy due to the potential well and keeps some of it after exiting. In the same way, the photon loses some energy entering and exiting a super-void. This is caused by a repulsive model of Dark energy causing expansion while the photon is travelling through the well or hill. The effect can be expressed as:

$$\frac{\delta T}{T}(\hat{n}) = - \int_{\eta_0}^{\eta_*} d\eta \frac{\partial(\Psi + \phi)}{\partial \eta} \quad (3.15)$$

Where η_* is conformal time, T is CMB temperature at a CMB surface and η_0 with an observer. We detect this by testing for a non-zero cross-correlation function between the number of galaxies per square degree and the temperature of CMB. The super-clusters heat the photons while the super-voids cool them.

The analysis of temperature anisotropies in CMB can also give an independent analysis for dark energies existence. The oldest sky we can see is the last scattering surface, which is where the electrons were trapped by hydrogen to form atoms (also known as the recombination or decoupling epoch. These photons were tightly coupled to baryons and electrons before decoupling where redshift was roughly 1090, after which, they could freely move. All matter components are coupled to gravity through Einstein's equations. The main source of the CMB temperature anisotropies comes from the scalar part of the perturbations. This is because, in an expanding universe, the vector perturbations will decay. The contribution made to CMB anisotropies from the tensor perturbations are as gravitational waves, the amplitude

of these are suppressed. If they originated from inflation, this becomes relative to the scalar perturbation from before.

Using the predicted temperature anisotropies

$$l(l+1)C_l(2\pi)^{-1} \quad (3.16)$$

versus l , the multi-pole moment, with 5 year observational data from WMAP, we can clearly see that the data observed matches with the theoretical power spectrum.

The angle measured θ has the relation $\theta = \frac{\pi}{l}(\text{rad})$. The larger scales link to lower values of l , the large scale power spectrum at $l < 10$ is dominated by the mono-pole mode. This shows almost scale invariant density perturbations which came from inflation. The reason we use (3.16) as our plot instead of C_l is because the equation is constant for scale invariant perturbations on large scales which means:

$$l(l+1)C_l = \frac{\pi}{2}\delta_H^2 \quad (3.17)$$

Where δ_H^2 is the amplitude of the curvature perturbations which came from inflation. [6, p. 35-36], [5, p. 12-13]

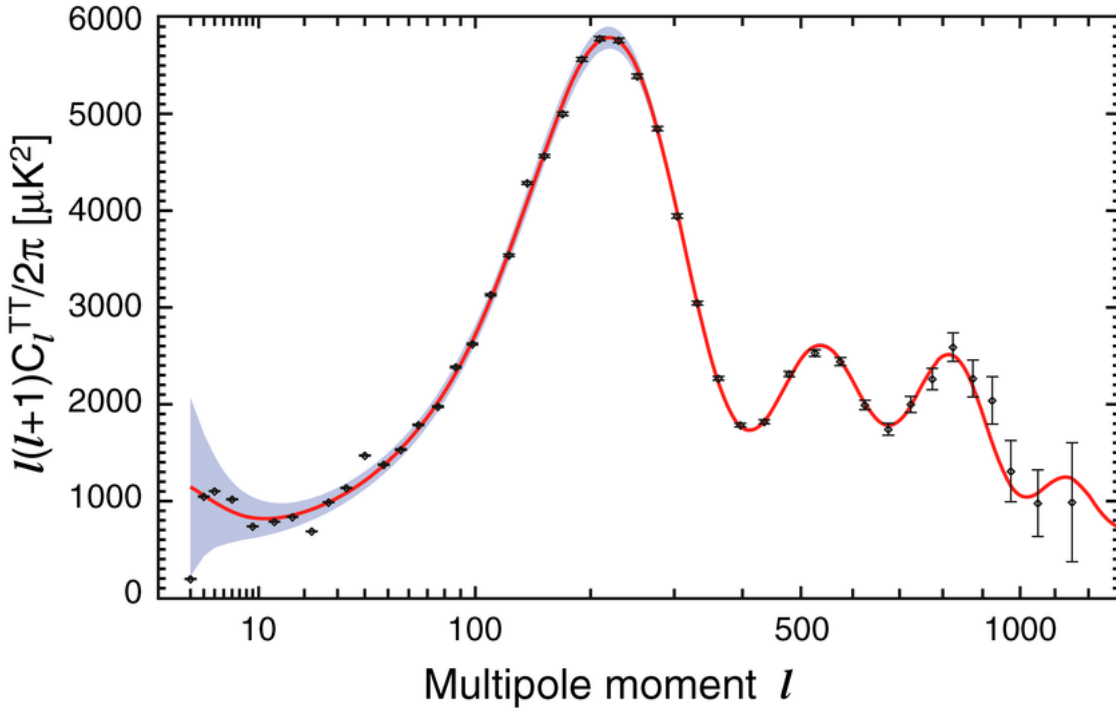


Figure 3.1: The CMB power spectrum versus the multiple moment and angular size. This curve shows the theoretical prediction of the power spectrum while the black points represent the WMAP data spanning across 5 years.

3.4 BAO

photons are coupled to baryon from before the decoupling epoch, baryon perturbations have the oscillations of sound waves imprinted in them. Along with the CMB temperature anisotropies. A peak was found for baryon acoustic oscillations in the large-scale correlation function at roughly $100h^{-1}Mpc$ separation, which was measured from a spectroscopic sample of roughly 45,000 red galaxies from the SDSS. This measurement gave us a new independent test for constraining the properties of dark energy.

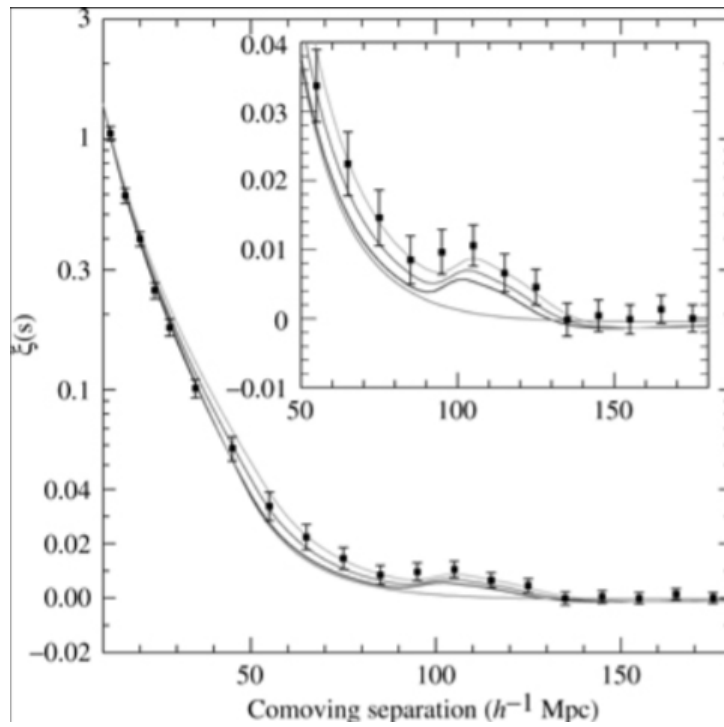


Figure 3.2: This graph displays the large scale redshift space correlation function of the SDSS sample of data. The smaller graph shows a zoomed-in version of the main graph, at the peak observed at $100h^{-1}Mpc$. From top to bottom, each curvature corresponds to $\Omega_m^{(0)}h^2 = 0.12, 0.13, 0.14$, with $\Omega_b^{(0)}h^2 = 0.024$. A pure CDM (baryon-less) model with $\Omega_m^{(0)}h^2 = 0.15$. The data clearly shows the acoustic peak around the stated separation distance.[1]

[3, p. 102-106]

3.5 Large-Scale Structure

We can get another test for dark energy by using the observations made on the large scale structure, like galaxy clustering.

The wavenumber at the peak position of $P_{\delta m}$ corresponds to k_{eq} decreases when $\Omega_m^{(0)}$ has smaller values. We can plot the predicted matter power spectrum for both a flat Λ CDM model where $\Omega_m^{(0)} = 0.28$, and the CDM model for which $\Omega_m^{(0)} = 1$. With dark energies existence, the peak position will shift toward a larger scale (for a smaller k). This means the peak position can be used to prove and probe dark energy.

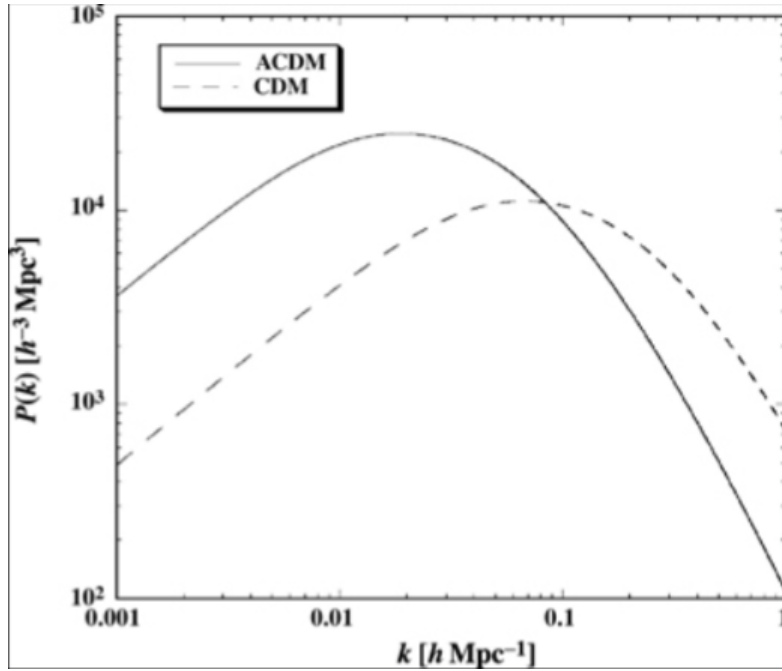


Figure 3.3: The predicted power matter power spectrum in the flat Λ CDM model, plotted along side the CDM model.

[3, p. 106-108] [5, p. 12-13]

4 Statistical Methods in Cosmology

4.1 The likelihood function

If we have a randomly generated variable x that represents the relative (apparent) magnitude for supernovae for example, has a probability distribution function $f(x; \theta)$ that depends on some unknown parameter, which could represent the absolute magnitude in our case, ' θ ' helps us differentiate between random variables, x , and the parameter θ . This kind of probability this is known as "a conditional probability of having the data x , given the theoretical parameter θ ". We can imagine that the relative (apparent) magnitude; m , has been distributed as a Gaussian like term with any known variance (being the observable error on m). We have:

$$m_{th} = 5 \log_{10} d_L(z; \Omega_m^0, \Omega_\Lambda^0) + C \quad (4.1)$$

Where C is a constant and d_L is the luminosity distance. by repeating the measurements and obtaining multiple values for x , we can use the law of joint probability to tell us the probability of obtaining the first x value in the interval dx_1 around x_1 , x_2 in the interval dx_2 around x_2 , x_3 and so forth. If the measures are independent of each other, this gives us:

$$f(x_i : \theta) d^n x_i = \Pi_i f_i(x_i : \theta) dx_i = f_1(x_1 : \theta) f_2(x_2 : \theta) f_3(x_3 : \theta) \dots dx_1 dx_2 dx_3 \dots \quad (4.2)$$

For every θ , this multivariate probability density function can take a different value. Therefore, It becomes sensible to call the best θ as the value for which our function is . If we make some randomly generated variables distributed as $f(x; \theta)$, the highest certainty outcome for x will be the value that maximises $f(x; \theta)$. If we have a specific outcome called x , our best idea becomes assuming that θ is such a term that's maximising the occurrence of that x outcome. We can define our best

θ_i as those that will maximise the joint function $(x_1, x_2 \dots x_n; \theta_1, \theta_2, \dots)$. In general we will have many parameters we have to estimate, so we can write the function simply as $f(x_i; \theta_j)$ which means all the x_i s and θ_j s

For the parameter equation, finding the parameters that will maximise the likelihood function $f(x_i; \theta_j)$ is the maximum likelihood method.

$$\frac{\partial f(x_i; \theta_j)}{\partial \theta_j} = 0, \quad j = 1, \dots, m \quad (4.3)$$

We can write these solutions for the equations with $\hat{\theta}_j$. They will act as functions of the data, which means they will be random variables, like the data is. The classical "frequentist" approach is trying to find the distribution of $\hat{\theta}_j$ s knowing the distribution of the x_j s. If this is attainable, we can give probabilities to our solutions range and try determine an interval of it that contains roughly 95% chance for the set of data being drawn from the theoretical distribution. Though, a problem is that alot of the time it's very hard to derive our solutions distribution analytically and difficult to derive these all numerically using simulated data sets. Another issue is this approach doesn't take consider what we already know about the theoretical parameters. To account for that information we have we must change to using the "Bayesian" approach. Rather than trying to look for the probability $f(x_j; \theta_j)$ of having the data given the model, we can determine the probability $L(\theta_j; x_i)$ of having the model given the data. Our Issue can then be dealt with by the theorem of conditional probability, Bayes theorem:

$$P(A; B) = \frac{P(B; A)P(A)}{P(B)} \quad (4.4)$$

We can say the the known data is x_i with B and the unknown theory, theoretical parameters θ_j , using A. The left hand side is the conditional probability of having the theory given the data. The conditional probability is represented by the right hand side of the equation, and is the probability of having our data given our theory. the probabilities $P(A)$ and $P(B)$ respectively represent the probabilities of having our theory and our data. Bayes theorem is a consequence of conditional probability itself, and the symmetry of the joint probability under the exchange of actions A and B. From this we can say:

$$L(\theta_j; x_i) = \frac{f(x_i; \theta_j)p(\theta_j)}{g(x_i)} \quad (4.5)$$

Where the $p(\theta_i)$ probability is called the prior probability for the parameter(s) θ_i , whereas $g(x_i)$ is the probability density function of the data x_i . The final function

which is $L(\theta_j; x_i)$ is known as the posterior probability. Although, sometimes it is called the likelihood and represented as L . The posterior contains the information we have been searching for: the probability distribution of the parameters given that we saw data x_i and that we have some kind of prior knowledge about the parameters themselves.

Since $L(\theta_j; x_i)$ is a probability distribution function for θ_j , we have to normalize it to unity:

$$\int L(\theta_j; x_i) d^n \theta_j = 1 = \frac{\int f(x_i; \theta_j) p(\theta_j) d^n \theta_j}{g(x_i)} \quad (4.6)$$

This means that:

$$\int f(x_i; \theta_j) p(\theta_j) d^n \theta_j = g(x_i) \quad (4.7)$$

The integral on the left hand side is referred to as "evidence" and sometimes, "evidence" can also be used to refer to $g(x_i)$. The function itself doesn't depend on the θ_i parameters which means it doesn't actually help estimate them. Normally, we do not know the probability distribution of theories, like whether the Λ CDM model is more probable than others, from an absolute point of view, then a model theorizing modified gravity. We do have some information that's independent of the data that we have. To be exact, we have the results from previously conducted experiments. If we have an experiment that can almost definitely exclude $\Omega_m^{(0)} < 0.1$, then this could be used by saying $p(\Omega_m^{(0)} < 0.1) = 0$. Instead, if we think that $h = 0.7 \pm 0.05$, we can use the mean of the Gaussian h as 0.7 as well as its standard distribution is 0.05. These are all examples of "prior distributions".

Prior distributions could be very flexible, to the point where you could simply exclude values like Ω_m^0 . All that matters is that it is stated, as every posterior will eventually become a prior.

Most of the time, we are working toward a set of parameters and regard others as "nuisance" parameters, and in a perfect world, we could just get rid of these parameters and be unaffected by their absence. For example, if we are trying to analyse data from supernovas relative (apparent) magnitudes, and putting them side by side for comparison to the expected values from theoretical predictions calculated from $m = 5 \log_{10} d_L(z; \Omega_m, \Omega_\Lambda) + C$, we would be very interested in the matter and cosmological constant density parameters, but not the constant C .

However, the constant C is dependent on the "K correction" and the absolute magnitude (M). The likelihood is then a function of C , as well as the other two

density parameters. However, we can change the function into one that only has the density parameters by removing C via integration:

$$L(\Omega_m, \Omega_\Lambda) = \int L(c, \Omega_m, \Omega_\Lambda) dC \quad (4.8)$$

This is marginalization. It is often used to reduce multidimensional problems down to a more manageable state. For example, if we had the maximum likelihood estimator of Ω_m as 0.3, and:

$$\int_R L(\Omega_m) d\Omega_m = 0.683 \quad (4.9)$$

Where R is the interval 0.1 to 0.4 of the mass density parameter, we can write our final result as $\Omega_m = 0.3^{+0.1}_{-0.2}$ at a 68.3% confidence level. [3, p. 356-363]

4.2 Fisher Matrix

A issue with our likelihood method is that we have to evaluate $L(\theta_i)$ for all θ_i . This can become a very long process when there are up to 10 parameters. If each calculation takes roughly 1 second this will take hundreds of years to fully evaluate...

One way to get around this is to apply the Monte Carlo approach. Rather than constructing a full grid, we can instead try explore random jumps. These jumps have sizes that can be related to the steepness of the function. This technique can grow with the number of parameters, but not on the same scale as the full grid method. A faster method is the Fisher Matrix, the method is to approximate a full likelihood with a multivariate Gaussian distribution:

$$L \approx N e^{-\frac{1}{2}(\theta_i - \hat{\theta}_i) F_{ij} (\theta_j - \hat{\theta}_j)} \quad (4.10)$$

Where the information/Fisher matrix F_{ij} represents the inverse of the correlation matrix and $\hat{\theta}_j$ and the maximum likelihood estimators are the functions of the data. We must remember that the likelihood is the Gaussian function of the parameters, not just the data as we often assume the data to be Gaussian but not the parameters themselves. If we expand the exponential in a normal and general likelihood near its peak, the maximum likelihood value $\hat{\theta}_i$ of the parameters, can be written as:

$$\ln(L\theta_i) \approx \ln(L\hat{\theta}_i) + \frac{1}{2} \frac{\partial^2 \ln L \theta_i}{\partial \theta_i \partial \theta_j} \bigg|_{ML} (\theta_i - \hat{\theta}_i)(\theta_j - \hat{\theta}_j) \quad (4.11)$$

Where ML means maximum likelihood. Because we are at a peak, the first deriva-

tives will vanish. We will find that the normalization $N = L(\hat{\theta}_i)$ will depend on the data, F_{ij} is written as:

$$F_{ij} = \frac{\partial^2 \ln L(\theta)}{\partial \theta_i \partial \theta_j} \Big|_{ML} \quad (4.12)$$

The Fisher matrix itself is defined as the expected value of the matrix which would be obtained by averaging the matrix over the data distribution:

$$F_{ij} = -\frac{\partial^2 \ln L(\theta)}{\partial \theta_i \partial \theta_j} = \int -\frac{\partial^2 \ln L(\theta)}{\partial \theta_i \partial \theta_j} L(x; \theta) dx \quad (4.13)$$

To find the ML estimator, we could use the Newton-Raphson method by making the guess that our parameter is close to $\theta^{(0)}$ and expanding the derivative of the logarithmic likelihood:

$$L_{,\theta}(\theta) = L_{,\theta}(\theta^{(0)}) + L_{,\theta\theta}(\theta - \theta^{(0)}) \quad (4.14)$$

And estimate the minimum of L by exploring $L_{,\theta}(\theta) = 0$ and then using:

$$\theta^{(1)} = \theta^{(0)} - \frac{L_{,\theta}}{L_{,\theta\theta}} \Big|_{\theta^{(0)}} \quad (4.15)$$

This is very fast for likelihood functions that are well behaved and can be generalized to multidimensional cases. One of the most useful applications of the Fisher formalism is when we don't need to look for our peak likelihood because we already know what our ML estimator is from the beginning. This can be the case when simulating an experiment. For example, if we want to simulate a future supernova experiment, which supposedly collects 10,000 light curves and find the peak magnitude with errors. we can begin by guessing that n random variables follow a probability distribution function with a known variables and mean $m_{th}(z_i; \Omega_m^{(0)}, \Omega_\Lambda^{(0)}) = 5 \log_{10} d_L(z_i; \Omega_m^{(0)}, \Omega_\Lambda^{(0)}) + C$. Here, we can take the PDF to be Gaussian but we can also assume another PDF type if we think it describes the data better. Since the data PDF is assumed to be Gaussian here, we can already form likelihood (we are also neglecting the normalization constant):

$$L_m \approx e^{-\frac{1}{2} \sum_i \frac{(m_i - m_{th}(z_i))^2}{\sigma_i^2}} = e^{(-\frac{1}{2} \mu_i C_{ij}^{-1} \mu_j)} \quad (4.16)$$

Where, to make things a little cleaner, we can use $\mu_i = m_i - m_{th}(z_i)$ as well as the correlation matrix C_{ij} which is simple for this case:

$$C = \text{diag}(\sigma_1^2, \sigma_2^2, \sigma_3^2) \quad (4.17)$$

When we are referring to dark energy, we are also interested in the parameters $\Omega_m^{(0)}, \Omega_\Lambda^{(0)}$. Because of this, we can produce a likelihood function of $\Omega_m^{(0)}, \Omega_\Lambda^{(0)}$, using the form of (4.10) to say:

$$L(\Omega_m^{(0)}, \Omega_\Lambda^{(0)}) = e^{\frac{1}{2}(\Omega_i^{(0)} - \hat{\Omega}_i^{(0)})F_{ij}(\Omega_j^{(0)} - \hat{\Omega}_j^{(0)})} \quad (4.18)$$

Where, again, the Fisher matrix is represented at F_{ij} , and the pair of i and j run over m and Λ . Since we don't have real data yet, we do not have actual maximum likelihood estimators. However, since we are estimating a future experiment, we can take the general values for these estimators $\Omega_m^{(0)} = 0.3, \Omega_\Lambda^{(0)} = 0.7$. However, this means that we will find the confidence regions only around this particular set of parameters. If we decide to change these values, we have to redo the calculations and all the results can potentially change in some way. The Fisher matrix of (4.16) is:

$$F_{ij} = \left. \frac{\partial \ln L_m}{\partial \Omega_i^{(0)} \partial \Omega_j^{(0)}} \right|_F = \Sigma \frac{1}{n \sigma_n^2} \left. \frac{\partial^2 m_{th}(z_n; \Omega_m^{(0)}, \Omega_\Lambda^{(0)})}{\partial \Omega_i^{(0)} \partial \Omega_j^{(0)}} \right|_F \quad (4.19)$$

The Fisher matrix F_{ij} is not diagonal even though the correlation matrix C_{ij} is. The same parameters are in all the means, we can change the chance of getting all m_i 's by changing the parameters.

As a final note on the $_{ij}$, the statistical theorem called the "Cramer-Rao inequality" says "the minimum variance of an unbiased estimator cant be less than F_{ii}^{-1} (first take the inverse then take the i-th term on the diagonal)". This means that the Fisher matrix gives the minimum error we could possibly obtain. The issue with this using this as an error estimate is that, for large samples, the estimators tend to be biased. [3, p. 367-376]

5 Dark Energy Constraints

5.1 parameterization of w_{DE}

Rather than writing the Hubble parameter using the redshift z , we can parametrize the equation of state for dark energy by using $H^2 = \frac{8G\pi}{3}(\rho_\phi + \rho_m)$ so that the Hubble parameter can instead be written as:

$$H^2(z) = H_0^2 \left[\Omega_m^{(0)}(1+z)^3 + (1 - \Omega_m^{(0)})f(z) \right] \quad (5.1)$$

Where we have:

$$f(z) = \frac{\rho_{DE}(z)}{\rho_{DE}^{(0)}} = e^{3 \int_0^z \frac{1+w(z)}{1+z} dz} \quad (5.2)$$

Therefore, $H(z)$ can be expressed when $w(z)$ is also parametrized. Then, we can observationally constrain the evolution of $w(z)$ using the relation $H(z) = \frac{d}{dz} \left(\frac{d_L(z)}{1+z} \right)^{-1}$

There are in fact a number of parameterizations of $w(z)$ which have been suggested so far. The Taylor expansion of $w(z)$ has frequently been used:

$$w(z) = \sum_{n=0} w_n x_n(z) \quad (5.3)$$

Where many expansion functions have been thought of:

Constant w : $x_0(z) = 1, x_n = 0, n \geq 1$

Redshift: $x_n(z) = z^n$

Scale factor: $x_n(z) = (1 - \frac{a}{a_0})^n = (\frac{1}{1+z})^n$

Log: $x_n(z) = (\log(1+z))^n$

The first case includes the Λ CDM mode. The second case was introduced with the Hubble parameter being:

$$H^2(z) = H_0^2 (\Omega_m^{(0)}(1+z)^3 + (1 - \Omega_m^{(0)})(1+z)^{3(1+w_0-w_1)} e^{3w_1 z}) \quad (5.4)$$

Thus, we can constrain the two parameters w_0 and w_1 by using supernova type Ia data. With the third case, at a linear order we have $w(z) = w_0 + w_1 \frac{z}{1+z}$ which was extended to a more general case:

$$w(z) = w_0 + w_1 \frac{z^P}{1+z^P} \quad (5.5)$$

For example, we have $w(\infty) = w_0 + w_1$ for $P = 1$ and $w(\infty) = w_0$ for $P = 2$. This difference is present for larger z while also being dependent on the value of P . Taylor expansions taken to the linear order for the other cases.

The two parameters, w_0 and w_1 can also be observationally constrained. An alternative approach allowed for tracker solutions where a quick evolution in the equation of state (meaning a evolution at the speed that the conventional power-law characteristic couldn't cause)

meant that a wide amount of quintessence models were able to be recreated in a fashionable way.

We can also use this discriminate between dynamic models of dark energy through the normalizing of the dark energy power spectrum (at cluster scales). We can also use this to observe evidence of quintessence in the CMB through the varied Integrated Sachs-Wolfe effect.

This approach is known as the "Kink" approach and can be expressed as a 4 parameter parameterization:

$$w(a) = w_0 + (w_m - w_0)\Gamma(a, a_t, \Delta) \quad (5.6)$$

Where Γ is the transition function that depends on a, a_t, Δ . In our case, a_t is the value of the scale factor at the transition point between $w = w_m$, which is the value in the matter-dominated era, and $w = w_0$ which is the value today. Δ controls the width of the transition. The transition function itself can be written in the general form as:

$$\Gamma(a, a_t, \Delta) = \frac{1 + e^{\frac{a_t}{\Delta}}}{1 + e^{\frac{a_t - a}{\Delta}}} \frac{1 - e^{\frac{1-a}{\Delta}}}{1 - e^{\frac{1}{\Delta}}} \quad (5.7)$$

The reason this is advantageous is because it can cope with very quick evolution of the equation of state, which is something difficult to see with the Taylor expansions earlier. [5, p. 62-63]

5.2 Supernova Ia data

The kink formula (5.6) yields the best-fit values for the parameters $w_0, w_m, a_t, \ln(\Delta)$ as: -2.85, -0.41, 0.94, -1.52 with a χ^2 value of 172.8. This corresponds to the equation of state that is nearly constant for $z > 0.1$ and very quickly decreases to $w = w_0$ for $z < 0.1$. This can be best shown with the following graph displaying the $z, w(z)$ relation.

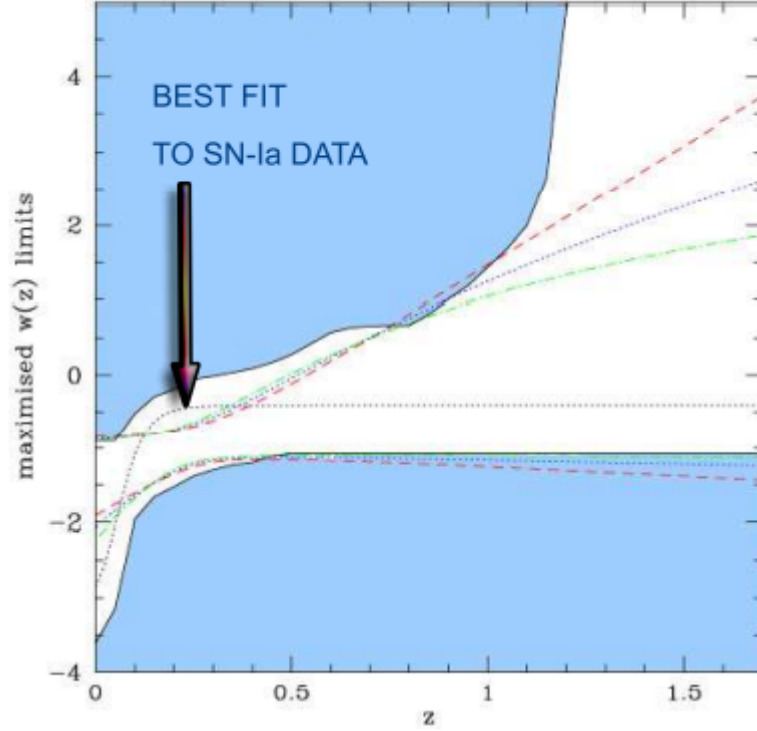


Figure 5.1: Plot displays the evolution of the equation of state for dark energy for the best-fit of the Kink parameterization. The maximised limits on $w(z)$ are displayed as redshift: the red dashed line, scale factor: green dashed and dotted line, logarithmic: blue dotted line, Kink: solid black lines

We can see that the best fit solution passes outside of the limits of all the Taylor series expansions for $0.1 < z < 0.3$ and $z < 0.1$. This could suggest that Taylor expansion at a linear order aren't sufficient to use when we have such a quick evolution of $w(z)$. It was found that the redshift for a universe as it enters an accelerating stage heavily depends on the parameterization of $w(z)$. The Λ CDM model has this redshift at 0.66 ± 0.11 which stays true to the equation:

$$z < z_c = \left(\frac{2\Omega_{\Lambda}^{(0)}}{\Omega_m^{(0)}} \right)^{\frac{1}{3}} - 1 \quad (5.8)$$

With $w(z) = w_0 + w_1 z$ we find z_c to be $0.14_{-0.05}^{+0.14}$ and $z_c = 0.59_{-0.21}^{+8.91}$ for the scale

factor parameterization of: $w(z) = w_0 + \frac{w_1 z}{(1+z)}$. These large differences in z_c can be used to distinguish the cosmological constant from dynamic dark energy models, however this has created unsurety about whether the standard two-parameter parameterizations in terms of w_0 and w_1 should be used.

By including higher order terms ($n > 2$) in the Taylor expansion, this problem can be solved to a certain degree. It was found that the allowed ranges for w_0 are shifted towards smaller values with a maximum likelihood of $w_0 = -4$. In addition, much larger values such as $w_1 = 50$ and $w_2 = -100$ are not forbidden.

These results display that the observational constraints on the equation of state for dark energy are sensitive to the parameterization of it and that we must have at least three parameters to fully address a wide range of the variation of the equation of state.

Something we could ask ourselves is how many parameters for dark energy do we need to describe the dynamics of dark energy? This can be answered by using the Akaike Information Criterion and the Bayesian Information Criterion. These two criteria can be defined as:

$$AIC = -2\ln(L) + 2k_p \quad (5.9)$$

$$BIC = -2\ln(L) + k_p \ln(N) \quad (5.10)$$

Where we have L as the maximum value of the likelihood, k_p represents the number of parameters and N is the number of data points we have. The optimal model will minimize the AIC or BIC. Typically, in the limit of large N , the AIC tends to favour models with more parameters while the BIC model does not. The BIC model gives us estimates for the posterior evidence of a model, under the assumption that there is no prior information. The BIC model becomes a useful approximation to make when we have a full evidence calculation with no prior set on the models. The minimum value of the BIC corresponds to the Λ CDM model. The simplest dark energy model with one parameter is typically preferred over the dynamic dark energy models. This is quite similar to the early universe inflation where single field models are liked more than multi-field models. [5, p. 63-65]

5.3 Constraints on CMB

Temperature anisotropies in CMB are expanded in spherical harmonics, The CMB spectrum can be written in the form:

$$C_t = 4\pi \int \frac{1}{k} dk P_{ini}(k) |\Delta_l(k, \eta)|^2 \quad (5.11)$$

Where $P_{ini}(k)$ is an initial power spectrum and $\Delta(k, \eta_0)$ is the transfer function for l multipoles of the k -th wavenumber at a present time η_0 where this is the conformal time, meaning $\eta_0 = \int a^{-1} dt$. The initial power spectrum is almost scale-invariant, which is consistent with the prediction of inflationary cosmology. The dynamic evolution of dark energy can affect the CMB temperature anisotropies in, at the very least, 2 different ways. Firstly, the position of the acoustic peak depends on the dark energies dynamics because of the angular diameter distance (which is related to the form of $w(z)$). Secondly, the CMB anisotropies are also affected by the Integrated Sachs-Wolfe effect.

To fully grasp the effect of the varying positions in the acoustic peaks, we can begin with the constant equation of state w for dark energy. The presence of dark energy also induces a shift by a linear factor s in the l -space positions of the acoustic peaks. The shift can be mathematically expressed as:

$$s = \sqrt{\Omega_m^{(0)}} D \quad (5.12)$$

Where D is the angular diameter distance, which can be expressed as:

$$D = \int_0^{z_{dec}} \frac{1}{\sqrt{\Omega_m^{(0)}(1+z)^3 + \Omega_{DE}^{(0)}(1+z)^{3(1+w)}}} dz \quad (5.13)$$

Where z_{dec} represents the redshift at decoupling. We can also express the transfer function as the sum of the last scattering surfaces contribution, as well as the Integrated Sachs-Wolfe effects contribution.

The ISW effects contribution can be expressed as:

$$\Delta_l^{ISW}(k) = 2 \int d\eta e^{-\tau} \frac{d\Psi}{d\eta} j_l(k(\eta - \eta_0)) \quad (5.14)$$

Where τ represents the optical depth because of the scattering of the photons, Ψ is the gravitational potential, and j_l represent the Bessel functions. The gravitational potential is constant in the matter-dominated period which in turn, means there is an absence of the ISW effect. This is important for large scale perturbations that

correspond to $l < 20$. In specific coupled dark energy models, we can see strong impacts on the CMB spectrum. [5, p. 63-65]

5.4 The cross Correlation

Another way to measure dark energy evolution with weak lensing was by developing a cross correlation technique using lensing tomography. The idea here is that they we could make use of the changes in the weak lensing shear with redshift for some massive foreground object, like (very) luminous galaxies. It depends only on the ratios of the angular diameter distances. Using massive foreground halos, we can compare high linear shear values in the same part of the sky. This allows us to eliminate one of the bigger sources of systematic error in cosmological weak lensing measurements.

When the cross correlation method is combined with the standard lensing tomography, which also possess complementary degeneracy's, we could argue that it would allow measurement of dark energy parameters with a much better accuracy then we have previously had.

The constraints on the quintessence models where the acceleration was driven by a slow-rolling scalar field have been explored, focusing mainly on the cosmic shear, combined with data from type Ia supernovae and CMB data. We have combined the quintessence models with computation of weak lensing observable, and have determined several 2-point shear statistics with data that includes the "golden set" of type Ia supernova data, aswell as CMB and large scale structure data. The baryon oscillations in the power spectrum of the galaxy functions can also constrain dark energies nature. Before the decoupling epoch, the universe was a hot plasma of photons, baryons, electrons and dark matter. The coupling with the photons and electrons due to Thompson scattering led to oscillations in the plasma. As the universe expanded and cooled, electrons and protons became atoms which caused the acoustic oscillations to stop, but they also became imprinted on the radiation aswell as on the baryons and can be seen in the spectrum of galaxy correlations at present.

The detection of these imprints of the oscillations in the galaxy correlation function is not easy as the signal is suppressed by the fractional energy density of the baryons, which is about 4%. Therefore, a high volume of the universe is required in order to detect such a signature. The imprints of baryon oscillation have recently been observed at SDSS. A peak in the correlation function was located at roughly

$100h^{-1}hMpc$ separation. Because of this, measuring the ratio of distance has at redshifts 0.35 to 1089 with a high accuracy is possible. From CMB radiation, it is possible to constrain the angular diameter distance at a redshift of $z = 1089$ for fixed $\Omega_m^{(0)}h^2$ and $\Omega_b^{(0)}h^2$ values. With a flat model at a constant cosmological constant, the distance only depends on the energy fraction of the cosmological constant. That means these measurements can be used to constrain the $\Omega_m^{(0)}$ and $\Omega_m^{(0)}h$ values to a good precision. Considering a flat model with an unknown equation of state (that isn't -1), gives us a two dimensional parameter space which requires more information, even with the CMB acoustic scale.

The measurements of baryon oscillations cant say anything about dark energy. The dynamic equation of state $w(z)$ would need extra information coming from large scale structure, like the observation on baryon oscillations at a higher value of redshift which is something we are still trying to obtain. [5],[2]

6 Models

6.1 Cosmological Constant

The cosmological constant is the simplest form of dark energy due to its energy density being constant across time and space. The Einstein tensor $\nabla_\nu G^{\mu\nu} = 0$ and energy conservation $\nabla_\nu T_{\mu\nu} = 0$. The $g^{\mu\nu}$ metric is constant w.r.t covariant derivatives ($\nabla_\alpha g^{\mu\nu} = 0$), we are able to $\Delta g_{\mu\nu}$ into the Einstein equations. The new equation becomes:

$$R_{\mu\nu} - \frac{1}{2}g_{\mu\nu}R + \Delta g_{\mu\nu} = 8\pi GT_{\mu\nu} \quad (6.1)$$

We can then take the trace of this equation and find that $-R + 4\Delta = 8\pi GT$, which allows us to rewrite it as such:

$$R_{\mu\nu} - \Lambda g_{\mu\nu} = 8\pi G \left(T_{\mu\nu} - \frac{1}{2}Tg_{\mu\nu} \right) \quad (6.2)$$

The famous fine tuning problem surrounding the cosmological constant arises from the fact that it needs to be of the order of the square of the present Hubble parameter

$$\Lambda = H_0^2 = (2.13h \cdot 10^{-42} GeV)^2 \quad (6.3)$$

This then sets the critical density to roughly:

$$\rho_\Lambda = \frac{\Lambda m_{pl}^2}{8\pi} = 10^{-47} GeV^4 \quad (6.4)$$

This is odd since the vacuum energy density evaluated at the zero-point energies of quantum fields with mass m is given by:

$$\rho_{vac} = \frac{1}{2} \int_0^\infty \frac{d^3k}{(2\pi)^3} \sqrt{k^2 + m^2} \quad (6.5)$$

Quantum field theory is only valid to a cut-off point, so the upper bound of the integral can be replaced with k_{max} where $k_{max} \gg m$. Since the integral is dominated

by k , we find that:

$$\rho_{vac} = \frac{k_{max}^4}{16\pi^2} \quad (6.6)$$

We can now say $k_{max} = m_{pl} = 1.22 \cdot 10^{19} GeV$ which gives us a value of:

$$p_{vac} = 10^{74} GeV^4 \quad (6.7)$$

This value is about 10^{121} times larger then the value we received earlier. Since we cant just get rid of the vacuum energy term, we can try cancel it by introducing other terms. The issue with this is that it requires ρ_λ to be fine tuned so that its present energy density of the universe. One theory is super symmetry. In super symmetric theories every bosonic degree of freedom has its Fermi counter part which contributes to the zero point energy with an opposite sign compared to the bosonic which cancels the vacuum energy. perfect Supersymmetry wants an equal number of fermionic and bosonic degrees of freedom for a given value of mass which makes the vacuum energy vanish, which means supersymmetric theories typically don't have the cosmological constant set to 0 since it breaks down at high enough energies (roughly $10^3 GeV$) so again, vacuum energy is normally above 0 with broken supersymmetry.

Another issue with the cosmological constant model is that its value is nearly exactly the same as value for present matter energy density. The matter density $\rho_m = \rho_m^{(0)}(1+z)^3$ links with the cosmological density $\rho_\Lambda^{(0)}$ at:

$$z_{link} = \left(\frac{\Omega_\Lambda^{(0)}}{1 - \Omega_\Lambda^{(0)}} \right)^{\frac{1}{3}} - 1 \quad (6.8)$$

Setting $\Omega_\Lambda^{(0)} = 0.7$, we receive $z_{link} = 0.3$. This is the coincidence problem. An interesting note is that most dark energy models also feature this coincidence problem and their z_{link} is also very close to 0. One explanation for this problem is that there is no coincidence, which could mean that Ω_m and Ω_{DE} behave similarly. Another explanation is the "back-reaction" argument. The coincidental relation between ρ_m and ρ_{DE} may be the cause of a different fundamental interesting relation, for example, the relation between structure formation and acceleration. A way where this makes sense is if one were case were to cause the other, for example; if structures growing causes the acceleration with both cumulative and non-linear effects.

[5, p. 13-18][3, p. 109-113]

6.2 Dark Energy models with Scaling Solutions

We've seen that models with quintessence scalar fields with exponential potentials have scaling solutions. We state that the equation of state is a constant and the fluid density and field density relation (ρ_M and ρ_ϕ) as such:

$$\frac{\rho_\phi}{\rho_M} = \text{constant} \neq 0, w_\phi = \text{constant} \quad (6.9)$$

With a model like this, the solution exists at a boundary between deceleration and acceleration. The shallower scalar field potential has solutions that exhibit tracking characteristics. Solutions that scale can also be found when dark energy couples with matter. If we start with a general action:

$$S = \int d^4x \sqrt{-G_M} \left[\frac{1}{2} R + P(\phi, X) \right] + S_m(g_{\nu\mu}, \phi, \Psi_m^{(i)}) \quad (6.10)$$

Where $P(\phi, X)$ is the Lagrangian density which is a function of the scalar field g_M is the determinant of the metric. The form of coupling shown in (6.31) is what we can assume for this case. This coupling can be assumed to be a function of the field. Of the solutions that exist, we use the one with a constant equation of state parameter that can be expressed as $w_\phi = \frac{P(\phi, X)}{\rho_\phi}$.

With a scaling idea, we assume that the universe is composed with 2 components: Matter with a 0 pressure (pressureless matter) which also has a 0 equation of state ($w_m = 0$), and a scalar field ϕ . From (6.25), we can use the energy densities to fulfil the equations of motion in a flat FLRW spacetime:

$$\frac{d\rho_\phi}{dN} + 3(1 + w_\phi)\rho_\phi = -Q(\phi)\rho_m \frac{d\phi}{dN} \quad (6.11)$$

$$\frac{d\rho_m}{dN} + 3(1 + w_m)\rho_m = +Q(m)\rho_m \frac{d}{dN} \quad (6.12)$$

Where $N = \ln(a)$. The Friedmann equation is then:

$$3H^2 = \rho_\phi + \rho_m \quad (6.13)$$

We can show the fractional densities for ρ_m and ρ_ϕ as:

$$\Omega_\phi = \frac{\rho_\phi}{3H^2}, \Omega_m = \frac{\rho_m}{3H^2}, \quad (6.14)$$

This will satisfy the sum of fractional densities relation (the sum of the fractional densities must be 1). [3, p. 214-225]

6.3 Quintessence

Quintessence represents a model of dark energy that features an ordinary scalar field and a potential that's minimally coupled to gravity (ϕ and $V(\phi)$ respectively). It interacts with all the other components through only gravity. Quintessence can be modelled as such:

$$S = \int d^4x \sqrt{-g} \left[-\frac{1}{2}(\nabla\phi)^2 - V(\phi) \right] \quad (6.15)$$

$$(\nabla\phi)^2 = g^{\mu\nu} \partial_\mu \phi \partial_\nu \phi \quad (6.16)$$

In the flat FRW spacetime:

$$\ddot{\phi} + 3H\dot{\phi} + \frac{dV}{d\phi} = 0 \quad (6.17)$$

Where our fields energy momentum tensor can be derived by changing (6.15) in terms of $g^{\mu\nu}$:

$$T_{\mu\nu} = -\frac{2}{\sqrt{-g}} \frac{\delta S}{\delta g^{\mu\nu}} \quad (6.18)$$

$$T_{\mu\nu} = \partial_\mu \phi \partial_\nu \phi - g \left[\frac{1}{2} g^{\alpha\beta} \partial_\alpha \phi \partial_\beta \phi + V(\phi) \right] \quad (6.19)$$

From this, we can obtain expressions for energy density and pressure of the field:

$$\rho = \frac{1}{2}\dot{\phi}^2 + V(\phi), P = \frac{1}{2}\dot{\phi}^2 - V(\phi) \quad (6.20)$$

And thus, the equation of state for Quintessence in a flat FRW universe:

$$w_\phi = \frac{P_\phi}{\rho_\phi} = \frac{\dot{\phi}^2 - 2V(\phi)}{\dot{\phi}^2 + 2V(\phi)} \quad (6.21)$$

The energy density ρ_M dominates over quintessence during matter or radiation dominated epochs. This means ρ_ϕ would track ρ_M , which allows dark energy density to emerge at later times of the universe. The tracking behaviour itself depends on the form of the potential. We see that if the potential is steep, $\frac{\dot{\phi}^2}{2} \gg V(\phi)$ is always satisfied. The equation of state is then $w_\phi \approx 1$ which means the energy density of the field will evolve $\rho_\phi = ka^{-6}$ which will decrease much faster than the background fluid density. To see late time cosmic acceleration, we need the condition $w_\phi < -\frac{1}{3}$.

This gives us $\dot{\phi}^2 < V(\phi)$. This means that the scalar potential must be shallow enough for the field to slowly evolve along the potential. By introducing the slow roll parameters:

$$\epsilon = \frac{m_{pl}^2}{16\pi} \left(\frac{dV}{Vd\phi} \right)^2, \eta = \frac{m_{pl}^2}{8\pi} \left(\frac{d^2V}{Vd\phi^2} \right) \quad (6.22)$$

we can expect inflation if $\epsilon \ll 1$ and $|\eta| \ll 1$ are satisfied. When referring to dark energy, the slow roll conditions are not always trustworthy. This is because we have dark matter as well as dark energy. They still serve as good measurements to check the existence of a solution with accelerated expansion. In essence, Quintessence is a dynamic model of dark energy, in that it changes with time. It can be attractive or repulsive depending on the ratio of kinetic and potential energy. Models of quintessence have a tracker like trait. It's field has a density that tracks the radiation density until radiation-matter equity. There is also a special form of Quintessence called "Phantom Energy". This form is a hypothetical version of dark energy which satisfies $w < -1$. This means it possesses negative kinetic energy. If this type of energy existed, the universe would likely end in a "big rip". This is where the space between subatomic particles expands too quickly and everything is essentially ripped apart. However the idea of phantom energy itself is usually dismissed as because it suggests that the vacuum is unstable with negative mass particles bursting into existence. Phantom Energy will be further expanded on in a later section.

[3, p. 135-138] [5, p. 20]

6.4 K-Essence

While Quintessence leans heavily on the potential energy of the scalar fields, which leads to acceleration of the universe at late times. It is possible to for a scenario to exist where the accelerated expansion arises from modifications to the kinetic energy of the scalar fields. Kinetic energy driven inflation - K inflation proposed to explain the early universes inflation at high energies. This was then applied to dark energy to form K essence. K essence is generally characterized by a scalar field with non-canonical kinetic energy. Using the Lagrangian density $p(\phi, X)$ and $X = -\frac{1}{2}(\nabla\phi)^2$, we can model it's action:

$$S = \int d^4x \sqrt{-g} p(\phi, X) \quad (6.23)$$

where the Lagrangian density corresponds to the pressure density. Using (35), we can find an expression for the energy momentum tensor of the scalar field:

$$T_{\mu\nu}^\phi = -\frac{2}{\sqrt{-g}} \frac{\delta(\sqrt{-g}P)}{\delta g^{\mu\nu}} \quad (6.24)$$

The energy momentum tensor of k essence is similar to a perfect fluid, where $T_{\nu\mu} = (\rho + P)u_\mu u_\nu + g_{\nu\mu}P$ with a velocity of $\mu_\mu = \frac{\partial_\mu \phi}{\sqrt{2X}}$, pressure $P_\phi = P$ and energy density $\rho_\phi = 2XP_X - P$ which finally, gives us the equation of state for K essence:

$$w_\phi = \frac{P_\phi}{\rho_\phi} = \frac{P}{2XP_X - P} \quad (6.25)$$

So long as the $2XP_X \ll P$ condition is satisfied, w_ϕ can be somewhat close to -1.

Within K essence, we can have a field known as a phantom field or a ghost scalar field if the kinetic energy has a negative sign (in X). Without higher order terms in ϕ or X, it would be hindered by the quantum instability problem. In the ghost condensate case, we can steer away from this quantum instability by the existence of the term X^2 . We can derive the stability conditions of K essence by taking small fluctuations $\delta\phi(t, x)$ around a background value $\phi_0(t)$, which is the solution in FLRW spacetime. We can decompose the field to obtain:

$$\phi(t, x) = \phi_0(t) + \delta\phi(t, x) \quad (6.26)$$

Since we are interested in UV instabilities, it's not restrictive to imagine a Minkowski background here. We can expand $P(\phi, X)$ at the second order in $\delta\phi$. We can also find the Lagrangian and the Hamiltonian for the fluctuations. The perturbed Hamil-

tonian is as follows:

$$\delta H = (P_X + 2XP_{XX})\frac{(\delta\dot{\phi})^2}{2} + P_X\frac{(\nabla\delta\phi)^2}{2} - P_{\phi\phi}\frac{(\delta\phi)^2}{2} \quad (6.27)$$

In cosmological perturbation theory, the speed of sound often appears as a coefficient of $\frac{k^2}{a^2}$. Here, k represents the comoving wavenumber while a represents the scale factor.

To interpret classic fluctuations as stable when we have a positive speed of sound, the quantum fluctuations stability must follow the conditions: $P_X + 2XP_{XX} > 0$ and $-P_{\phi\phi} > 0$.

If those conditions aren't met, our vacuum will become unstable because of the production of ghost and photon pairs. These conditions are therefore what prevent an instability with negative energy ghost states. We can explain the production rate from the vacuum because it is proportional to the phase space integral on all the final states possible.

Because only a UV cutoff will prevent the creation of modes of high energies, this is a UV instability. The phantom model with Lagrangian density violates both conditions stated earlier which means, again, that the vacuum is unstable.

[3, p. 172-177] [5, p. 20-22]

6.5 Phantom Fields

Observational data shows that the equation of state parameter lies inside a narrow strip around $w=-1$, and is more or less consistent with being below this value. When the equation of state is less than -1, dark energy is typically referred to as a phantom dark energy, or ghost dark energy. There are specific models of Brans-Dicke scalar tensor gravity theories that can lead to this. The simplest explanation for phantom dark energy is given by imagining a scalar field with negative kinetic energy.

Phantom fields were originally introduced as a version of steady state theory. After refining the theory behind the Phantom dark energy idea, the action of the phantom field minimally coupled to gravity can be expressed as:

$$S = \int d^4x \sqrt{-g} \left[\frac{1}{2} (\nabla \phi)^2 - V(\phi) \right] \quad (6.28)$$

Where the kinetic terms sign is opposite compared to kinetic terms from actions given by an ordinary scalar field. Using the equation of state formula, we can express w_ϕ as:

$$w_\phi = \frac{p}{\rho} = \frac{\dot{\phi}^2 + 2V(\phi)}{\dot{\phi}^2 - 2V(\phi)} \quad (6.29)$$

The curvature of the universe will grow toward infinity with a finite time passed in the universe dominated by a phantom fluid. In this case, we would typically expect a big rip singularity however, it can actually be avoided if the potential is as follows:

$$V(\phi) = V_0 \left[\cosh\left(\frac{\alpha\phi}{m_{pl}}\right) \right]^{-1} \quad (6.30)$$

Because of the peculiar properties of the phantom field, the field will evolve toward to the top of the potential and cross over the other side. It will turn back to a period of damped oscillations about the maximum of the potential at $\phi = 0$. After a set amount of time, the motion will cease and the field will settle at the top of the potential to mimic the de-sitter behaviour, which means $w_\phi = -1$. The behaviour of phantom fields is interesting as classical cosmological field. However, its riddled with ultra violet quantum instabilities, since the energy density of the phantom fields are unbound from below, the vacuum will become unstable against the production of both ghost and normal fields. Even when ghosts become decoupled from matter fields, they will couple to gravitons instead which will mediate vacuum decay process that have the: $\text{vacuum} \rightarrow 2\text{ghosts} + 2\gamma$ type. Finally, it was shown that we need an awkward Lorentz invariance breaking term with a cut off, of an order

around MeV to prevent the overproduction of cosmic gamma rays. This means the origin of the phantom field is still a challenge.

Since the energy density of dark energy is of similar order to that of the dark matter in the universe, it is not unreasonable to assume a potential relation between the two. One theory proposes that interaction between dark matter and quintessence of the form $Q\rho_m\dot{\phi}$. This kind of interaction appears in scalar-tensor theories like the Brans-Dicke theory. In the B-D theory, the coupling with the Ricci scalar R and the scalar field ϕ give way to a constant coupling Q (in an Einstein frame) between non relativistic matter and ϕ . We can consider interactions between the scalar field and non relativistic matter by saying:

$$\nabla_\mu T_{v(\phi)}^\mu = -QT_M \nabla_v \phi, \nabla_\mu T_{v(M)}^\mu = QT_M \nabla_v \phi \quad (6.31)$$

In this case, $T_{v(\phi)}^\mu$ and $T_{v(M)}^\mu$ are the energy-momentum tensors of non relativistic matter and ϕ . The trace of the matter fluid is $T_M = -\rho_M + 3p_M$. The coupling terms vanish since radiation is trace-less. The coupling strength (Q) of baryons is generally different from dark matter. If we make the assumption that baryons are completely uncoupled then we also assume they follow geodesics. This means we can analyse the results with the observations as this is what we experimentally assume. We can also state that the frame where the baryons follow the geodesics is the "physical" frame, which further indicates that the results are directly comparable with the observations. The Lagrangian field density of the coupled quintessence is $L_\phi = -\frac{1}{2}g^{\mu\nu}\partial_\mu\phi\partial_\nu\phi - V(\phi) + L_{int}$ where L_{int} gives rise to the interacting energy-momentum tensor in (40). The field potential can take the exponential form:

$$V(\phi) = V_0 e^{-\lambda\phi} \quad (6.32)$$

Though it is possible to choose a different form. Without losing the generality, we can assume that the λ constant is positive. For the interactions in (40), the field, radiation and non relativistic matter, in the flat FLRW background, will obey the following equations:

$$\dot{\rho}_\phi + 3H(\rho_\phi + P_\phi) = -Q\rho_m\dot{\phi} \quad (6.33)$$

$$\dot{\rho}_m + 3H\rho_m = +Q\rho_m\dot{\phi} \quad (6.34)$$

$$\dot{\rho}_r + 4H\rho_r = 0 \quad (6.35)$$

along with the normal Friedman equation:

$$3H^2 = \rho_\phi + \rho_m + \rho_r \quad (6.36)$$

Using equation of state identities, we can rewrite (42) as:

$$\ddot{\phi} + 3H\dot{\phi} + V_\phi = -Q\rho_m \quad (6.37)$$

To examine the dynamics of this system, we can introduce the following 3 variables:

$$x_1 = \frac{\dot{\phi}}{\sqrt{6}H}, x_2 = \frac{\sqrt{V}}{\sqrt{3}H}, x_3 = \frac{\sqrt{\rho_r}}{\sqrt{3}H} \quad (6.38)$$

By taking the derivative of the Friedman equation (45) in terms of the number of e-folds (N), together with (42-45), we obtain the following:

$$\frac{dH}{HdN} = \frac{-1}{2}(3 + 3x_1^2 + 3x_2^2 + 3x_3^2) \quad (6.39)$$

Where the effective equation of state is then:

$$w_{eff} = x_1^2 - x_2^2 + \frac{x_3^2}{3} \quad (6.40)$$

From this, the equation of state w_ϕ and the density parameter Ω_ϕ of the scalar field are obtainable:

$$w_\phi = \frac{x_1^2 - x_2^2}{x_1^2 + x_2^2}, \Omega_\phi = x_1^2 + x_2^2 \quad (6.41)$$

We can now discuss models where non-relativistic matter couples to dark energy. These models have energy density ρ_X and equation of state w_X . The interaction between these follows the conservation equations:

$$\dot{\rho}_m + 3H\rho_m = +\Gamma\rho_m \quad (6.42)$$

$$\dot{\rho}_X + 3H(1 + w_X)\rho_X = -\Gamma\rho_m \quad (6.43)$$

Γ represents the strength of the coupling. We can measure Γ in terms of the hubble parameter H and define the dimensionless coupling:

$$\delta = \frac{\Gamma}{H} \quad (6.44)$$

Here, a positive δ shows a transfer of energy from dark energy to dark matter,

whereas a negative δ tells us the opposite. Our aim is to find observational bounds on δ . So long as we only cosmic distance whose upper limits of the redshift are smaller than roughly 1000, we can ignore radiation and still have a good approximation. (6.42) can be rewritten to show:

$$\rho_m = \rho_m^{(0)} \frac{a^{-3}}{a_0} e^{\int \delta d(\ln(a))} \quad (6.45)$$

The Cosmological evolution can vary depending on the coupling form δ .

6.5.1 Constant δ Models

For models with a constant coupling form, (6.45) can be integrated to show:

$$\rho_m = \rho_m^{(0)} (1+z)^{3-\delta} \quad (6.46)$$

If the equation of state, w_X is also constant, we can substitute (6.46) into (6.43). Still neglecting radiation and using the Friedman equation, we have:

$$\frac{H(z)}{H_0} = \Omega_X^{(0)} (1+z)^{3(1+w_x)} + \frac{1 - \Omega_X^{(0)}}{\delta + 3w_X} \left[\delta (1+z)^{3(1+w_z)} + 3w_x (1+z)^{3-\delta} \right] \quad (6.47)$$

With this equation, we have 3 parameters that describe the Hubble parameter $(\delta, w_X, \Omega_X^{(0)})$. From here we can cross reference our data from type 1a supernovas, CMB and BAO observations with the theoretical values given by the equation. Using this, we can put observational constraints on δ from the data of: luminosity distance of type 1a supernovae, CMB shift parameter and the BAO effective distance.

6.5.2 Varying δ Models

To find $H(z)$ for a varying δ , one method is to assume the following relation:

$$\frac{\rho_X}{\rho_m} = \frac{\rho_X^{(0)}}{\rho_m^{(0)}} \left(\frac{a}{a_0} \right)^\xi \quad (6.48)$$

Where ξ is a constant. If this constant is 0, (6.48) will show the scaling relation between dark energy and dark matter. The existence of the interaction between dark energy and dark matter shows that $\xi = / = -3w_X$. If we take a time derivative of (6.48) and substitute (6.42) and (6.43) into it, we obtain an expression for the dimensionless coupling δ :

$$\delta(z) = -(\xi + 3w_X)\Omega_X(z) \quad (6.49)$$

Where $\Omega_X(z) = \frac{\rho_X}{3H^2}$. The density parameter itself is given by:

$$\Omega_X(z) = \left[\frac{\rho_m^{(0)}}{\rho_X^{(0)}}(1+z)^\xi + 1 \right]^{-1} \quad (6.50)$$

The coupling also varies in time, following the equation:

$$\delta(z) = \frac{\delta_0}{\Omega_X^{(0)} + (1 - \Omega_X^{(0)})(1+z)^\xi} \quad (6.51)$$

where the coupling $\delta_0 = -(\xi + 3w_X)\Omega_X^{(0)}$ represents the present value of the coupling. While $\xi > 0$, from the equation we can see the coupling will get smaller for higher z . Using (6.42) and (6.43), with (6.48), we can get a differential equation for the total density ($\rho_T = \rho_m + \rho_X$). This differential can be integrated and used to express the evolution of the normalized Hubble parameter:

$$\frac{H(z)}{H_0} = (1+z)^3 \left[1 - \Omega_X^{(0)} + \Omega_X^{(0)}(1+z)^{-\xi} \right]^{\frac{-3w_X}{\xi}} \quad (6.52)$$

This equation is based around the same three parameters ($\xi, w_X, \Omega_X^{(0)}$). Because δ_0 is related to these variables with the equation:

$$\delta_0 = -(\xi + 3w_X)\Omega_X^{(0)} \quad (6.53)$$

We can have the three parameters vary when we execute a likelihood analysis to test our model with observational data. The likelihood analysis using all the data from type 1a supernovae, the CMB shift parameter and the BAO effective distance (same data sources as constant δ models), give the bounds: $-0.4 < \delta_0 < 0.1, -1.18 < w_X < -0.91, 0.69 < \Omega_X^{(0)} < 0.77$ [3, p. 200]. The observational constraint is not as intense compared to the constant coupling model because $\delta(z)$ decreases for larger z .

The results we have obtained are based only on the changes of the background expansion history of the universe that came from coupling. These results state that we can say the coupling Λ CMB model aligns the data provided.

If we want to consider galaxy clustering (as an example), we need to look at the way matter density perturbation changes over time in the coupled dark energy models. We have seen that there is an instability of the matter perturbation in the radiation dominated epoch for the constant w_X models. The assumption of a

constant equation of state in itself is restrictive, so we could extend the analysis to more realistic models with a varying equation of state. However, the simple parameterization of the Hubble parameter becomes difficult, so it becomes easier to chase the possibility of avoiding instabilities in perturbations. [3, p. 189-200], [5, p. 44-50]

6.6 Tachyon Fields

It has been suggested that rolling tachyon condensates, in a class of string theories, could hold interesting cosmological consequences. It was showed that the decay of D-branes produces a pressureless gas with a finite energy density that is somewhat similar to dust. A rolling tachyon has a thought provoking equation of state who's parameter smoothly interpolates between 0 and -1. This led to many attempts in constructing a reasonable cosmological model using the tachyon as a candidate for the inflation at high energy. Tachyon inflation in open string models is usually surged with several difficulties associated with density perturbations and reheating. Tachyon can also act as a source of dark energy depending on the form of the tachyon potential. By considering the dynamics of the tachyon on a non unstable D3-brane, the 4D action is as follows:

$$S = - \int d^4x V(\phi) \sqrt{-\det(g_{\mu\nu} + \partial_\mu \phi \partial_\nu \phi)} \quad (6.54)$$

Where $V(\phi)$ is the tachyon potential. The effective potential from open string theory takes the form:

$$V(\phi) = \frac{V_0}{\cosh(\frac{\phi}{\phi_0})} \quad (6.55)$$

With $\phi_0 = \sqrt{2}$ for the non BPS D-branes in the super string and $\phi_0 = 2$ for bosonic strings. The tachyon has a ground state where ϕ approaches infinity. There are other potentials which appear as the excitation of massive scalar fields on the anti D branes. They have different potentials and have a minima where ϕ is set to 0. This potential is given by $V(\phi) = V_0 e^{\frac{1}{2}m^2\phi^2}$ and the potential has a minima where $\phi = 0$.

The energy momentum tensor from (6.54) takes the form:

$$T_{\nu\mu} = \frac{V(\phi) \partial_\mu \phi \partial_\nu \phi}{\sqrt{1 + g^{\alpha\beta} \partial_\mu \phi \partial_\nu \phi}} - g_{\nu\mu} V(\phi) \sqrt{1 + g^{\alpha\beta} \partial_\mu \phi \partial_\nu \phi} \quad (6.56)$$

For a flat FRW background, the energy density and pressure density are expressed as:

$$\rho = -T_0^0 = \frac{V(\phi)}{\sqrt{1 - \dot{\phi}^2}} \quad (6.57)$$

$$p = T_i^i = -V(\phi) \sqrt{1 - \dot{\phi}^2} \quad (6.58)$$

Using (2.3) and (2.1), we can find the equations of motion:

$$H^2 = \frac{8\pi GV(\phi)}{3\sqrt{1-\dot{\phi}^2}} \quad (6.59)$$

$$\frac{\ddot{\phi}}{1-\dot{\phi}^2} + 3H\dot{\phi} + \frac{dV}{Vd\phi} = 0 \quad (6.60)$$

Using these together gives:

$$\frac{\ddot{a}}{a} = \frac{8\pi GV(\phi)}{3\sqrt{1-\dot{\phi}^2}} \left(1 - \frac{3}{2}\dot{\phi}^2\right) \quad (6.61)$$

This means that we will see an accelerated expansion when $\dot{\phi}^2 < \frac{2}{3}$. The equation of state for the tachyon is:

$$w_\phi = \frac{p}{\rho} = \dot{\phi}^2 - 1 \quad (6.62)$$

The dynamics for the tachyon are different from a standard field case. Regardless of the steepness of the tachyon potential, the equation of state will vary from 0 to -1. In this case the tachyon energy density will behave as $\rho = ka^{-m}$ where $0 < m < 3$. This is because of the rewritten continuity equation (2.1):

$$\rho = \rho_0 e^{-\int 3(1+w_\phi) \frac{da}{a}} \quad (6.63)$$

where p_0 is an integration constant.

We can actually express $V(\phi)$ and ϕ in terms of H and \dot{H} , from (6.59) and (6.61), we find that $\frac{\dot{H}}{H^2} = (-\frac{3}{2})\dot{\phi}^2$. Using this with (6.59) we find that:

$$V = \frac{3H^2}{8\pi G} \left(1 + \frac{2\dot{H}}{3H^2}\right)^{\frac{1}{2}} \quad (6.64)$$

$$\phi = \int dt \left(-\frac{2\dot{H}}{3H^2}\right)^{\frac{1}{2}} \quad (6.65)$$

This means the tachyon potential will look like:

$$V(\phi) = \frac{2p}{4\pi G} \left(1 - \frac{2}{3p}\right)^{\frac{1}{2}} \phi^{-2} \quad (6.66)$$

Here, the evolution of the tachyon can be found by using $\phi = \sqrt{\frac{2}{3p}t}$, where the integration constant can be set to 0). The inverse square power law potential corresponds to a scaling solution. [5, p. 23-24]

6.7 Chameleon Scalar Fields

Let's say a scalar field were could couple to non-relativistic matter, similar to the coupled quintessence scenario, it then raises a fifth force interaction which can then be experimentally constrained. Coupling of the order of unity comes up in super-gravity and super-string theories. The Chameleon Mechanisms purpose was to solve large coupling models issue with local gravity constraints, the existence of strongly coupled scalar fields is generally incompatible with local gravity experiments without something suppressing the fifth forces propagation. This idea was revolving around some quintessence field whose effective mass was not the same depending on its surroundings. The maxima of the field potential that the field displays is because of the coupling matter. Provided the matter density is high enough as in the interior of a compact object, the field obtains a large mass around the potential minimum so it can't propagate freely. The field, in a low-density like the outer side of the same compact object, has a lighter mass. The chameleon Mechanism operates wherever a scalar field couples to matter in a way where the effective mass depends on the surrounding matter density. If the matter density is low, the scalar is light and can mediate a fifth force of gravitational strength. However, near the Earth where we can conduct experiments, the local density is high and a large mass is acquired. This makes it's effects short range and because of that, observable. Chameleon scalar fields control a fifth force of gravitational strength between matter particles, where the range can decrease when the ambient matter density increases. This means it avoids being detected in high density areas. The action for the chameleon scalar field ϕ with a potential of $V(\phi)$ is similar to the coupled quintessence:

$$S = \int d^4x \sqrt{-g} \left[\frac{1}{2} R - \frac{1}{2} g^{\nu\mu} \partial_\mu \phi \partial_\nu \phi - V(\phi) \right] - \int d^4x L_m(g_v^{(i)\mu}, \Psi_m^{(i)}) \quad (6.67)$$

Where g is the determinant of $g_{\nu\mu}$ in the Einstein frame, L_m is a matter Lagrangian with Ψ_m being the matter fields coupled to the metric $g_{\nu\mu}$. The metric is related to the Einstein frame metric $g_{\nu\mu}$ by:

$$g_{\nu\mu} = e^{2Q_i\phi} g_{\nu\mu} \quad (6.68)$$

Here, Q_i represents the strengths of the couplings for each matter component with field ϕ .

(6.67) originates from the theory where the field ϕ has a direct interaction of the form $e^{-2Q\phi} \tilde{R}$ with \tilde{R} (where \tilde{R} is the Ricci scalar). This fits into a class of scalar tensor theories where the action is generally given by:

$$\tilde{S} = \int d^4x \sqrt{-g} \left[\frac{1}{2} e^{-2Q\phi} \tilde{R} - \frac{1}{2} (1 - 6Q^2) e^{-2Q\phi} (\tilde{\nabla}\phi)^2 - U(\phi) \right] - \int d^4x L_m(\tilde{g}_{\mu\nu}, \Phi_m) \quad (6.69)$$

Tilde represents the quantities in a frame where ϕ has direct interaction with \tilde{R} (The Jordan frame). (6.69) is equal to that in Brans-Dicke theory with a potential $U(\phi)$. With a conformal transformation, (6.68), we can get the earlier action (6.67) in an Einstein frame along with field potential $V(\phi) = U(\phi)e^{4Q\phi}$. The couplings are the same for each matter field and the metric in (6.67) refers to the metric in the Jordan frame.

The fifth force on any given test particle of unit mass and a coupling Q is given by $F_\phi = -Q\nabla\phi$. Therefore its amplitude in the region $r > r_c$ is:

$$F_\phi = 2|QQ_{eff}| \frac{GM_c}{r^2} \quad (6.70)$$

So long as $|Q_{eff}| \ll 1$, it becomes possible to suppress the fifth force relative to the gravitational force $\frac{GM_c}{r^2}$. The amplitude for the effective coupling can be made to be much smaller than $|Q|$ so long as the conditions $\delta r_c = r_c - r_1 \ll r_c$ and $m_A r_c \gg 1$ are followed. Therefore, the body must have a thin-shell and the field must be heavy inside the body for the chameleon mechanism to work.

[3, p. 204-215]

6.8 Chaplygin Gas

Another interesting scalar-field model of dark energy involves a fluid called Chaplygin gas. The fluid also leads to the acceleration of the universe at late times. In its simplest form, its equation of state is as follows:

$$p = \frac{-A}{\rho} \quad (6.71)$$

Where A is a positive constant and $p = \frac{-V(\phi)}{\rho}$ for the tachyon. The Chaplygin gas can be referred to as a special case of a tachyon with a constant potential. The equation of state for the gas can be derived from the Nambu-Goto for a D-brane moving in a $D + 1$ dimensional bulk. From the equation of state, the continuity equation can be integrated to obtain:

$$\rho = \sqrt{A + \frac{B}{a^6}} \quad (6.72)$$

Where B is constant. Then we can find the following asymptotic behaviours:

$$\rho \sim \frac{\sqrt{B}}{a^3}, a \ll \left(\frac{B}{A}\right)^{\frac{1}{6}} \quad (6.73)$$

$$\rho \sim \sqrt{A}, a \gg \left(\frac{B}{A}\right)^{\frac{1}{6}} \quad (6.74)$$

where a is the scale factor. At early times where a is small, the gas behaves similarly to a pressureless dust. However, it becomes much more similar to the cosmological constant at later times which leads to an accelerated expansion. We can obtain the corresponding potential for the Chaplygin gas by treating it as if it was an ordinary scalar field ϕ . Using the equation of state and the integrated continuity equation together with $\rho = \frac{\dot{\phi}}{2} + V(\phi)$ and $p = \frac{\dot{\phi}}{2} - V(\phi)$, we find that:

$$\dot{\phi} = \frac{B}{a^6 \sqrt{A + \frac{B}{a^6}}} \quad (6.75)$$

$$V = \frac{1}{2} \left[\sqrt{A + \frac{B}{a^6}} + \frac{A}{\sqrt{A + \frac{B}{a^6}}} \right] \quad (6.76)$$

Since the Hubble expansion rate is $H = \frac{8\pi\rho}{3m_{pl}^2}^{\frac{1}{2}}$, we can rewrite our expression for $\dot{\phi}^2$ in terms of the derivative of a :

$$\frac{k}{\sqrt{3}} \frac{d\phi}{da} = \frac{\sqrt{B}}{a\sqrt{Aa^6 + B}} \quad (6.77)$$

Note, we are using $k^2 = 8\pi G = 1$. $\dot{\phi}^2$ in terms of the derivative of a can be integrated to give:

$$a^6 = \frac{4B^2\sqrt{3}k\phi}{A(1 - e^{2\sqrt{3}k\phi})^2} \quad (6.78)$$

which can then be substituted back into our equation for V to give:

$$V(\phi) = \frac{\sqrt{A}}{2} (\cosh(\sqrt{3}k\phi) + \frac{1}{\cosh\sqrt{3}k\phi}) \quad (6.79)$$

Therefore, a minimally coupled field with this kind of potential is equivalent to the Chaplygin gas model which gives an thought provoking possibility for the unification of dark energy and dark matter. However, it was shown that Chaplygin gas models experience strong observational pressure from CMB anisotropies. This comes from the fact that Jeans instability of perturbations in the Chaplygin gas models acts similarly to cold dark matter fluctuations in the dust-dominant stage, which we can see from our expression for density where $a \ll \frac{B^{\frac{1}{6}}}{A}$ but disappears when $a \ll \frac{B^{\frac{1}{6}}}{A}$. This suppression of perturbations and the existence of a non-zero Jeans length gives rise to a very strong ISW effect, which leads to the power loss in CMB anisotropies. [5, p. 26]

6.9 Unified Models of Dark Energy and Dark Matter

There have been many different theories to try and unify dark matter and dark energy. Whether it be using a single fluid or a scalar field

6.9.1 Generalized Chaplygin Gas

In the Chaplygin model, the energy density is inversely related to the pressure of the perfect fluid with $P = \frac{-A}{\rho}$. Generally speaking, we can also say:

$$P = -A\rho^{-\alpha} \quad (6.80)$$

In this equation, A is some non negative constant. If we find that the pressure is getting lower compared to the energy density in the early cosmological era, we can say that $\alpha > 0$.

However, at later times, cosmic acceleration occurs because of the negative pressure. A fluid with the Chaplygin equation of state will interpolate between pressureless matter and dark energy. In principle, it could replace both. Using (6.80) equation and our continuity equation (2.1), we obtain:

$$\rho(t) = \left[A + \frac{B}{a^{3(1+\alpha)}} \right]^{\frac{1}{1+\alpha}} \quad (6.81)$$

Here, $a(t) = (1+z)^{-1}$ is the scale factor but normalized to unity today and B is an integration constant. In (6.81), we can see the density ρ changes with $\rho = ka^{-3}$ during the early era where the scale factor $a \ll 1$ and as $p = ka^{\frac{1}{1+\alpha}}$ in the late epoch where the scale factor $a \gg 1$. In a flat FLRW background, the relation between density and expansion rate H is as follows:

$$3H^2 = 8\pi G\rho \quad (6.82)$$

Where we can introduce these following expressions:

$$p_* = (A + B)^{\frac{1}{1+\alpha}} \quad (6.83)$$

$$\Omega_m^* = \frac{B}{A + B} \quad (6.84)$$

Where Ω_m^* can be interpreted as an effective matter density (not to be confused with $\Omega_m^{(0)}$). (6.81) can now be written as:

$$\rho(z) = \rho_* \left[1 - \Omega_m^* + \Omega_m^* (1+z)^{3(1+\alpha)} \right]^{\frac{1}{1+\alpha}} \quad (6.85)$$

From here, we can make an expression for the equation of state:

$$w(z) = - \left[1 + \frac{\Omega_m^*}{1 - \Omega_m^*} (1+z)^{3(1+\alpha)} \right]^{-1} \quad (6.86)$$

In the region with high redshift, where $z \gg 1$, we approach the value $w \approx 0$. The present value of w is currently $w(0) = -(1 - \Omega_m^*)$. the equation of state will approach the value $w = -1$ in the future. Therefore, the generalized Chaplygin gas model can consider both dark matter and dark energy for the background level at least.

6.9.2 K-essence as a unified model

We can now consider a unified model using a field ϕ . We can do this using an only kinetic Lagrangian density:

$$P = F(X) \quad (6.87)$$

Where $F(X)$ is the function for kinetic energy, $X = -\frac{1}{2}g^{\mu\nu}\partial_\mu\phi\partial_\nu\phi$. The field energy density and pressure can be expressed as: $\rho_\phi = 2XF_X - F$ and $P_\phi = F$. The continuity equation in the flat FLRW time can then give:

$$(F_X + 2XF_{XX})X + 6HF_XX = 0 \quad (6.88)$$

which can then be integrated to give:

$$XF_X^2 = Ca^{-6} \quad (6.89)$$

Where C is the integration constant. We can take the function $F(x)$ with a max at $X = X_0$, so that $F_X(X_0) = 0$. This means:

$$F(X) = F_0 + F_2(X - X_0)^2 \quad (6.90)$$

Where F_0 and F_2 are constants. We can then find the solution for (6.88) using the condition:

$$\epsilon = \frac{X - X_0}{X_0} \ll 1 \quad (6.91)$$

If we substitute (6.90) into (6.88) we can find a linear order equation for ϵ that looks like:

$$\dot{\epsilon} = -3H\epsilon \quad (6.92)$$

Which can give us the following solution for X :

$$X = X_0 \left[1 + \epsilon_1 \frac{a^{-3}}{a_1} \right] \quad (6.93)$$

Where ϵ_1 and a_1 are constants. For our previous condition to be valid, we must have:

$$\epsilon \frac{a^{-3}}{a_1} \ll 1 \quad (6.94)$$

This means that the solutions approach the maxima at $X = X_0$ where $F_X(X_0) = 0$. The field energy density can then be given by:

$$\rho_\phi \approx -F_0 + 4F_2 X_0^2 \epsilon \frac{a^{-3}}{a_1} \quad (6.95)$$

Where we can neglect the term higher than $\epsilon_1 \frac{a^{-3}}{a_1}$. For the positivity of the energy density we must have $F_0 < 0$. The equation of state of K essence is:

$$w_\phi = \frac{P_\phi}{\rho_\phi} = - \left[1 + \frac{4F_2}{-F_0} X_0^2 \epsilon_1 \frac{a^{-3}}{a_1} \right]^{-1} \quad (6.96)$$

Which will eventually approach the de sitter value where $w_\phi \rightarrow -1$ at late times, this also means $\epsilon_1 \frac{a^{-3}}{a_1} \rightarrow 0$. The results are only valid under the previous conditions. However, it is also possible to have $w_\phi \approx 0$ in the matter-dominated era if the condition $\frac{4F_2 X_0^2}{-F_0} \gg 1$ is met. [3, p. 225-230]

6.10 Future Singularities

With GR, if the EoS (equation of state) is less than -1, we will continue until it reaches a big-rip singularity, meaning the universe itself with this property has a finite lifetime. The big rip singularity is called a "Type I singularity". This outcome can be seen in the Phantom Energy model of Dark energy. This scenario relates to breaking the null energy condition: $\rho + P > 0$. This singularity would exhibit the following behaviour:

$$Type I : a \rightarrow \infty, \rho \rightarrow \infty, |P| \rightarrow \infty \text{ as } t \rightarrow t_s \quad (6.97)$$

Where t_s is simply time of singularity. There are also different types of future singularities that appear at a non-infinite time, even if the null energy condition is not broken. There is a immediate future singularity that can be described as when:

$$Type II : a \rightarrow a_s, \rho \rightarrow \rho_s, |P| \rightarrow \infty \text{ as } t \rightarrow t_s \quad (6.98)$$

There are more singularities such as:

$$Type III : a \rightarrow a_s, \rho \rightarrow \infty, |P| \rightarrow \infty, \text{ as } t \rightarrow t_s \quad (6.99)$$

$$Type IV : a \rightarrow a_s, \rho \rightarrow 0, |P| \rightarrow 0 \text{ as } t \rightarrow t_s \quad (6.100)$$

If we imagine a fluid where its density ρ and pressure P have the following relation:

$$P = -\rho - f(\rho) \quad (6.101)$$

Where $f(\rho)$ is a function with respect to density ρ . The functions first potential form $f(\rho) = k\rho^\alpha$ was considered within the context of inflationary cosmology. Using (6.101) and the continuity equation (2.1), we can find the scale factor, which is given by:

$$a = a_0 e^{\frac{1}{3} \int \frac{1}{f(\rho)} d\rho} \quad (6.102)$$

Where a_0 is a constant. If the fluid with the equation of state (6.101) exists in a flat FLRW background universe then the $3H^2 = k^2\rho$ term has to be dominant so that the cosmic time t can be expressed as:

$$t = \int \frac{1}{k\sqrt{3\rho f(\rho)}} d\rho \quad (6.103)$$

So that we can show an example of the type II singularity, we can take the

function:

$$f(\rho) = A(\rho_0 - \rho)^{-\gamma} \quad (6.104)$$

Where A , ρ_0 and $\gamma(> 0)$ are all constants. In the limit $\rho \rightarrow \rho_0$, we have $|P| \rightarrow \infty$ because of the divergence in $f(\rho)$. From (6.102), the scale factor will evolve to be:

$$a = a_0 e^{\frac{-(\rho_0 - \rho)^{\gamma+1}}{3A(\gamma+1)}} \quad (6.105)$$

Which means that $a \rightarrow a_0$ while $\rho \rightarrow \rho_0$. The Hubble parameter: $H = \frac{\dot{a}}{a} = k\sqrt{\rho}$ is then finite, so that \dot{a} also remains finite. Meanwhile, the second derivative of the scale factor, \ddot{a} is divergent as $\rho \rightarrow \rho_0$ because of the divergence of the pressure P . The equation of state is given by:

$$w = \frac{P}{\rho} = \frac{A}{\rho(\rho_0 - \rho)^\gamma} \quad (6.106)$$

Which means $w > -1$ for $A < 0$ and $0 < \rho < \rho_0$. This means that a sudden singularity is present even when we are considering non-phantom dark energy ($w > -1$)

In order to consider the type III singularity, we must take the following function:

$$f(\rho) = B\rho^\alpha \quad (6.107)$$

Where B and α are constants. From (6.102), we can find that:

$$a = a_0 e^{\frac{\rho^{1-\alpha}}{3(1-\alpha)B}} \quad (6.108)$$

we also find that:

$$t = t_s + \frac{2(\rho^{-\alpha+\frac{1}{2}})}{\sqrt{3kB}(1-2\alpha)} \quad (6.109)$$

$$t = t_s + \frac{\ln(\rho)}{\sqrt{3kB}} \quad (6.110)$$

When $\alpha > 1$ the scale factor will be finite, even for $\rho \rightarrow \infty$. Meanwhile, when $\alpha < 1$, we have $a \rightarrow \infty$ as $\rho \rightarrow \infty$ for $B \neq 0$. If $\alpha > \frac{1}{2}$, the divergence of ρ will occur at the time t_s . Although, if $\alpha < \frac{1}{2}$ ρ diverges in the infinite past or future. Because the equation of state for dark energy is given by the expression $w = -1 - B\rho^{\alpha-1}$, it makes sense to say that $w > -1$ for $B < 0$. Thus, we can now class the types of singularities based on the following conditions:

1. $\alpha > 1$

There is a type III singularity with $w > -1$ for $B < 0$

2. $\frac{1}{2} < \alpha < 1$

There is a type I singularity in the future with $w < -1$ for $B > 0$. When $B < 0$, the scale factor approaches 0 as the density approaches infinity. Therefore, if the singularity exists in the future, we call the singularity the Big Crunch singularity.

3. $0 < \alpha < \frac{1}{2}$

There is no future singularity in this case.

It has been shown that the type IV singularity is present for the following function:

$$f(\rho) = \frac{AB\rho^{\alpha+\beta}}{A\rho^\alpha + B\rho^\beta} \quad (6.111)$$

We say that the Ricci scalar $R = k^2(\rho - 3P)$ diverges as $t \rightarrow t_S$ for type I,II and III singularities. In these cases, higher-order curvature terms would be as important as R blows up.

As a final note, we also identify Type II as a "sudden" singularity is one that takes a finite time to form (an example of this concept is that, for outside observers, black holes take an infinite amount of time to form). While the Type I singularity is a "Big Rip" singularity, which is where space expands too fast for fundamental forces to keep up with, and everything, even down to subatomic particles are ripped apart. This type of singularity would be present if Phantom Energy was the best fit model of dark energy due to its equation of state being less than -1. Luckily for us, Phantom Energy as a model for dark energy in our universe is (currently...) far from the best fit.

[3, p. 230-233], [5, p. 69-70], [8]

7 Conclusion

Dark energy is the driving force behind the acceleration of the universe, and is both a thrilling and challenging field for physicists to work on. The number of theories and intricacies within the field is extraordinary and as time goes on, it is very likely that many more will emerge. In fact, even the technology to acquire data that helps us create these ideas is evolving itself. Along with the analysis of such data. Writing a review on such a topic has been incredibly challenging due to its complex nature. Covering all the mathematics and all the theories is near impossible which makes a true review of dark energy as a whole a daunting task. Upon inspection, it is very easy to argue that the cosmological constant model fits the best. However, we still have the task of explaining the coincidence problem behind it, and why it has only become relevant very recently. Interestingly enough, we have begun using Gamma Ray Bursts as standard candles, due to their increased luminosity compared to the norm; Type Ia supernovae. Theoretically, they could be viewed to redshifts of roughly $z \sim 10$ which would give us a much more detailed Hubble diagram, and thus a more accurate analysis of whether the equation of state is evolving. From the data we have, it is actually reasonable to argue that a dynamic equation of state is the best fit! This inherently opposes everything we have currently believed (about the cosmological constant being the best fit model for dark energy). While the proof for this is statistically insignificant (for the time being), it would be fun to play with the idea that, like nature, dark energy evolves aswell. [5, p. 80]

Bibliography

- [1] *Cosmology Results from eBOSS* *Cosmology Implications from SDSS BOSS and eBOSS*. SDSS. URL <https://www.sdss.org/science/cosmology-results-from-eboss/>.
- [2] *Planck 2015 results. XIV. Dark energy and modified gravity*. Feb 2015. URL <https://arxiv.org/abs/1502.01590>.
- [3] L. Amendola and S. Tsujikawa. *Dark Energy: Theories and Observations*. Nature, Institute of Theoretical Physics University of Heidelberg Tokyo University of Science, June 2010. ISBN 9780521516006.
- [4] Astronomy Section Rochester Academy of Science. *Bright Supernovae - 1998*. URL <https://www.rochesterastronomy.org/snimages/sn1998.html>.
- [5] E. J. Copeland, M. Sami, and S. Tsujikawa. *Dynamics of Dark Energy*. Nature, University Park Nottingham NG7 2RD United Kingdom Centre for Theoretical Physics Jamia Millia Islamia New Delhi India Department of Physics Jamia Millia Islamia New Delhi India Department of Physics Gunma National College of Technology Gunma 371-8530 Japan, Feb 2008. URL <https://arxiv.org/abs/hep-th/0603057>.
- [6] M. Ishak. *Testing General Relativity in Cosmology*. Nature, Dec 2018. URL <https://doi.org/10.1007/s41114-018-0017-4>.
- [7] Miao Li and Xiao-Dong Li and Shuang Wang and Yi Wang. *Dark Energy*. Institute of Theoretical Physics, Chinese Academy of Sciences Beijing 100190, China Kavli Institute for Theoretical Physics, Key Laboratory of Frontiers in Theoretical Physics Beijing 100190, China Department of Modern Physics, University of Science and Technology of China Hefei 230026, China Physics Department, McGill University Montreal, H3A2T8, Canada, march 2011. URL <https://arxiv.org/abs/1103.5870>.
- [8] S. Nojiri, S. D. Odintsov, and S. Tsujikawa. *Properties of singularities in (phantom) dark energy universe*. Nature, Department of Applied Physics National Defence Academy Hashirimizu Yokosuka 239-8686 Japan Instituci'o Catalana de Recerca i Estudis Avancats (ICREA) and Institut d'Estudis Espacials de Catalunya (IEEC) Edifici Nexus Gran Capit'a 2-4 08034 Barcelona Spain Department of Physics Gunma National College of Technology Gunma 371-8530 Japan, Feb 2008. URL <https://arxiv.org/abs/hep-th/0501025>.